Inclusive D-meson and Λ_c Production in Two Photon Collisions at LEP

M. Chapkin*, V. Obraztsov*, A. Sokolov*

*Institute for High Energy Physics, 142284 Protvino, Moscow Region, Russia

Abstract. The inclusive production of D^{*+}, D^0, D^+ and Λ_c is measured by DELPHI in photon-photon collisions at LEP-II energies. The measured cross sections are compatible with the QCD calculations having the contributions from the resolved processes sensitive to the gluon density in photon. The total cross section of the charm quark production in two-photon collisions at LEP-II energies is estimated.

INTRODUCTION

Hadron production in two-photon collisions is described by the Vector meson Dominance Model (VDM) [1], the Quark Parton Model (direct process) (QPM) [2], and the hard scattering of hadronic constituents of quasi-real photons (resolved photon process)[3-7]. Charm quark production in $\gamma\gamma$ collisions has several advantages over light quark production as a test of QCD. First, the theoretical QCD calculations are less ambiguous since charm quark has a large mass compared with the typical mass scale for strong interactions. Secondly, in charm quark production the VDM contributions are small, and only the direct quark-parton model and resolved photon processes have to be considered. Studies of charm meson production might provide usefull information about the gluon density in the photon, the current charm quark mass, and the intrinsic p_T distribution of partons in resolved photons.

Fig. 1 shows some of the diagrams contributing to heavy quark production in two-photon physics. The diagram in Fig. 1a shows the direct (QPM) process in which the photon couples directly to a quark. The diagram in Fig. 1d shows the single resolved photon process.

CP571, *PHOTON 2000,* edited by A. J. Finch

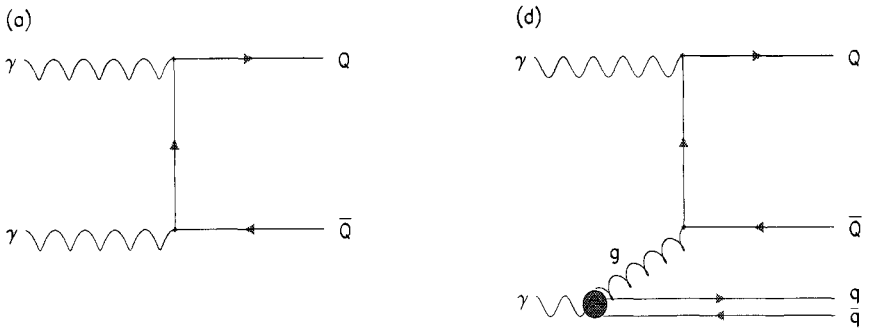

FIGURE 1. Examples of diagrams contributing to heavy quark production in $\gamma\gamma$ collisions. (a) Direct process (QPM); (d) single "resolved" process.

The direct process is dominant at low energies. However a large contribution from the resolved photon processes is predicted at high energies ($\sqrt{s_{ee}} \geq 200$ GeV) [8,9].

The charm production in $\gamma\gamma$ collisions was studied by measuring the D^{*+}, inclusive electron (muon) and K^0_s production by JADE [10], TPC/Two-Gamma [11], TASSO [12], TOPAZ [13,14], VENUS [15] and AMY [16]. Results from LEP were recently reported by ALEPH [17], L3 [18] and OPAL [19].

In this paper we report on measurement of charm production in $\gamma\gamma$ collisions at LEP-II energies via the inclusive production of D^{*+}, D^0, D^+ mesons and Λ_c[1]. D^{*+} mesons were detected by their decay to $D^0\pi^+$, with the D^0 observed in the decay modes (1) $K^-\pi^+$, (2) $K^-\pi^+\pi^-\pi^+$ and (3) $K^0_s\pi^+\pi^-$. Inclusive D^0 and D^+ mesons were detected by their decays to $K^-\pi^+$ and $K^-\pi^+\pi^+$, respectively. Λ_c's were detected by the decays to $pK^-\pi^+$, $\Lambda\pi^+\pi^-\pi^+$, pK^0_s, $pK^0_s\pi^+\pi^-$, $pK^-\pi^+\pi^0$, $\Lambda\pi^+\pi^0$.

EXPERIMENTAL PROCEDURE

The data obtained by DELPHI detector [20,21] in 1996-1999 were used. The energies of e^+e^- collisions, and the corresponding integrated luminosities $\int Ldt$ are presented in Table 1.

TABLE 1. Integrated luminosities.

Year	96		97	98	99					Σ
$\sqrt{s_{ee}}$, GeV	161	172	183	189	192	196	200	202	204	
$\int Ldt$, pb^{-1}	10.2	10.2	54.1	157.6	25.9	76.4	83.4	40.6	0.04	458.4

Our analysis is based on the selection of a low background sample of hadronic two-photon events. Several selection criteria for charged tracks and neutral particles

[1] Throughout this paper charge conjugate decays are implicitly included.

in an event were applied. Charged particle tracks in the detector were accepted if the following criteria were met:

- transverse particle momentum $p_T > 100$ MeV/c;
- impact parameter of a track transverse to the beam axis $\Delta_{xy} < 3$ cm;
- impact parameter of a track along the beam axis $\Delta_z < 10$ cm;
- polar angle of a track $21° < \theta < 159°$;
- track length $l > 30$ cm;
- relative error of the track momentum $\Delta p/p < 100\%$.

To select neutral particles the calorimetric information was used. Those calorimeter clusters which are not associated to the charged particle tracks are used to form the signals from neutral particles (γ, π^0, K^0_L, n). The following thresholds were chosen for measured energy: 0.3 GeV for the showers in the electromagnetic calorimeters and 1 GeV in the hadron calorimeters.

To extract the hadronic two-photon events, the following cuts were applied to the full sample:

- visible invariant mass calculated from the four-momentum vectors of the measured charged and neutral particles is $W_{vis} < 52$ GeV/c^2;
- number of charged particles $4 \leq N_{ch} \leq 16$;
- the sum of the transverse energy components with respect to the beam direction of all charged and neutral particles is $\sum E_T^{vis} > 3$ GeV/c;
- TPC and RICH detectors were fully operational.

The last requirement reduces the integrated luminosity for the analysis to 434.1 pb^{-1}.

A comparison of the W_{vis} distributions for the data and simulated events in Fig. 2 shows that the cut $W_{vis} < 52$ GeV/c rejects the main part of non two-photon events.

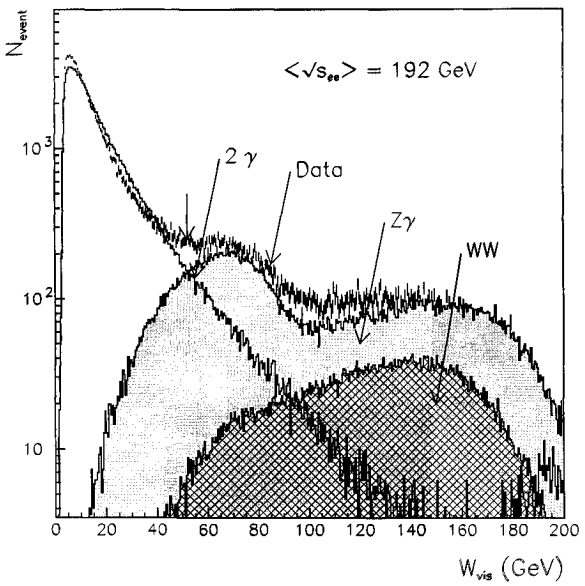

FIGURE 2. W_{vis} distributions for the data at $< \sqrt{s_{ee}} >= 192$ GeV and for the simulated $\gamma\gamma \rightarrow$ *hadrons*, $e^+e^- \rightarrow Z^0\gamma$ and $e^+e^- \rightarrow W^+W^-$ events at $\sqrt{s_{ee}} = 200$ GeV

The condition $4 \leq N_{ch} \leq 16$ decreases the combinatorial background for inclusive D mesons and Λ_c detection.

To obtain a sample of hadronic two photon events enriched in charm quark events with trigger efficiency $\geq 98\%$ [22], the additional cut was applied:

- at least one charged track from the barrel part of an event, i.e. with $45° < \theta < 135°$, has $p_T > 1.2$ GeV/c.

116323 events were selected after applying the above cuts.

The main background is from the $e^+e^- \rightarrow Z^0\gamma$ process and amounts to ~3.1% of the selected $\gamma\gamma$ events. The backgrounds from the $e^+e^- \rightarrow W^+W^-$ and other processes are negligible.

In order to compare the data with the theoretical predictions, samples of $\gamma\gamma \rightarrow q\bar{q}$ events simulated by TWOGAM [23] and PYTHIA 5.7 [24] programs were used. The simulated events were processed through the full chain of the DELPHI detector simulation and reconstruction programs.

As we will see below the observed distributions of charm states are well described by both generators. To compare with the other experiments we used PYTHIA.

D^{*+} PRODUCTION

D^{*+} mesons are detected by their decay into $D^0\pi^+$. The method of their reconstruction exploits the small mass difference between D^{*+} and D^0 mesons. The available kinetic energy of the π meson in the rest frame of the decay $D^{*+}\rightarrow D^0\pi^+$ is only 6 MeV and as a result the distribution of the variable $\Delta M = M_{D^{*+}} - M_{D^0}$ has a narrow peak. The signal is displayed by plotting ΔM for all reconstructed decay product candidates. D^0 mesons are identified via their decays to $K^-\pi^+$, $K^-\pi^+\pi^-\pi^+$and $K^0_s\pi^+\pi^-$.

To select D^0 candidates in the $K^-\pi^+$, $K^-\pi^+\pi^-\pi^+$ decay modes, the following additional criteria were applied for the charged tracks:

- the impact parameters of the track are $\Delta_{xy} < 0.5$ cm and $\Delta_z < 2$ cm;
- the particle should not be identified as a muon;
- the particle should not be identified as a electron.

A good identification of the kaons is important for D^0 meson selection. With the Rich Imaging Cherenkov Chamber (RICH) DELPHI possesses a unique and very important hadron identification tool. The information from the liquid and gas radiators of RICH can be combined with the dE/dx information of the Time Projection Chamber (TPC) [20] to achieve separation of hadrons at different momenta.

The particle identification algorithms for the RICH and TPC detector are realised in the RIBMEAN and HADSIGN packages [25]. A package MACRIB [26] combines the benefits of RICH algorithms and dE/dx information for the high momentum region. The combination is done using a neural network, which has a much better performance than any of its input variables alone.

For separation of the signal (kaon tracks) from the background, the target of the net output x_K is set to 1 and -1 respectively. The output of the net for the data and Monte Carlo can be seen in Fig. 3. A clear separation of the kaons from background is observed. The MACRIB has a better performance than the RIBMEAN and HADSIGN packages. In addition, it is a more flexible tool as cuts can be performed as a continuous variable instead of taking discrete tags.

The charged particles satisfing the "loose" kaon criterion for $x_K > -0.5$ were used as kaon candidates for D^{*+} meson selection. All charged particles not identified as electron, muon or kaon were considered as pions.

For the D^0 selection, all combinations of two (for $K^-\pi^+$ decay mode) or four (for $K^-\pi^+\pi^-\pi^+$ decay mode) charged particles with the zero total charge and with one track identified as a kaon, were considered.

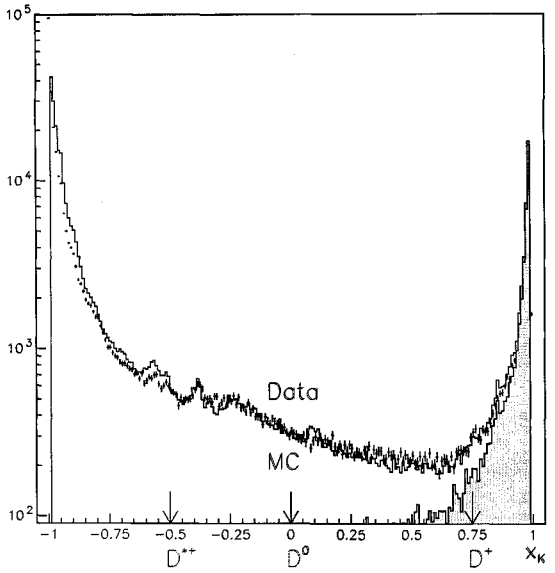

FIGURE 3. The output of the MACRIB kaon net for the charged tracks from the selected two photon events. The signal (output from kaon tracks) is accumulated at +1 (shaded area) and the background at -1.

The combination of an oppositely charged kaon and pion was considered as a candidate for the $D^0 \rightarrow K^-\pi^+$ decay if their invariant mass was within the range

$$1.83\ \mathrm{GeV/c^2} < M_{K^-\pi^+} < 1.90\ \mathrm{GeV/c^2}.$$

For the $D^0 \rightarrow K^-\pi^+\pi^-\pi^+$, the invariant mass was required to be in the range

$$1.85\ \mathrm{GeV/c^2} < M_{K^-\pi^+\pi^-\pi^+} < 1.88\ \mathrm{GeV/c^2}.$$

These ranges were determined from the resolution for $M_{K^-\pi^+}$, $M_{K^-\pi^+\pi^-\pi^+}$ observed in the full Monte Carlo simulation.

For the K^0_s in the $D^0 \rightarrow K^0_s\pi^+\pi^-$ channel, the standard DELPHI procedure of K^0_s reconstruction [21] was applied. To form $D^0 \rightarrow K^0_s\pi^+\pi^-$ candidates, all the combinations of the reconstructed K^0_s with two charged tracks with zero total charge identified as pions were used. The corresponding invariant mass was taken in the range

$$1.83\ \mathrm{GeV/c^2} < M_{K^0_s\pi^+\pi^-} < 1.90\ \mathrm{GeV/c^2}.$$

A particle identified as a π^+ is added to the $K^-\pi^+$, $K^-\pi^+\pi^-\pi^+$ or $K^0_s\pi^+\pi^-$ combinations from the above-mentioned mass ranges to form the D^{*+} candidate.

The resulting distributions of mass difference $\Delta M = (M_{\mathrm{D}^{*+}} - M_{\mathrm{D}^0})$ for different D^0 decay channels are shown in Fig. 4. A clear peak is observed around the D^{*+} and D^0 mass difference. Each histogram is fitted by the sum of a Breit-Wigner function and a background function $f(\Delta M) = \alpha \cdot (\Delta M - m_\pi)^\beta$. The distribution for the "wrong sign" combination of tracks is also shown with the pion used to form the D^{*+} from the D^0 required to have the same charge as the kaon. This produces a background spectrum from which the significance of the signal obtained from the right sign combination may be extracted. The significance of the signal for the $\mathrm{D}^0 \to \mathrm{K}^0_s\pi^+\pi^-$ decay was obtained from the fitting procedure. The numbers of the signal events $N_{\mathrm{D}^{*+}}$ for each D^0 decay mode are presented in the Table 2.

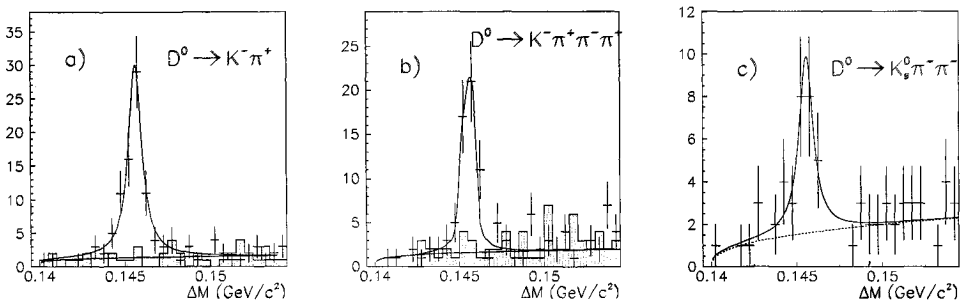

FIGURE 4. The distributions of the mass difference between the D^{*+} and D^0 for the $\mathrm{D}^0 \to \mathrm{K}^-\pi^+$(a), $\mathrm{K}^-\pi^+\pi^-\pi^+$(b), $\mathrm{K}^0_s\pi^+\pi^-$(c). The histograms are fitted by the sum of a Breit-Wigner function and the background function $f(\Delta M) = \alpha \cdot (\Delta M - m_\pi)^\beta$. The distributions for "wrong sign" combinations of tracks are shown by hatched histograms.

The D^{*+} production cross section is calculated as

$$\sigma^{\mathrm{D}^*} = \frac{N^{\mathrm{D}^*}_{exp}}{\varepsilon_{\mathrm{D}^*} \cdot L \cdot Br}$$

where $N^{\mathrm{D}^*}_{exp}$ is the observed number of D^{*+} mesons, $\varepsilon_{\mathrm{D}^*}$ is the reconstruction efficiency of D^{*+} in the corresponding mode, L is the integrated luminosity and Br is the branching ratio of D^{*+} decay to the corresponding decay chain.

The D^{*+} reconstruction efficiencies $\varepsilon_{\mathrm{D}^{*+}}$ for each D^0 decay mode calculated using PYTHIA are presented in the Table 2. Also we presented in the Table 2 the statistical uncertainties of $\varepsilon_{\mathrm{D}^{*+}}$ due to the limited number of MC events.

The main sources of systematic uncertainties are

- the branching fractions errors ($\sim$5%);
- uncertainties of reconstruction efficiency, determined by the changing of the PYTHIA model parameters: the p_T cut of the hard-scattering partons, the gluon density in the photon ($\sim$17%).

The systematic uncertainties are added in quadrature.

The calculated D^{*+} cross sections for different D^0 decay modes together with their weighted average are summarized in the Table 2.

TABLE 2. Calculation of the cross section of the process $e^+e^- \to e^+e^- D^{*+}X$.

D^0 decay mode	$K^-\pi^+$	$K^-\pi^+\pi^-\pi^+$	$K^0_s\pi^+\pi^-$
Branching fraction (%)	3.85 ± 0.09	7.6 ± 0.4	1.84 ± 0.14
$N_{D^{*+}}$	79 ± 11	54 ± 12	22 ± 7
$\varepsilon_{D^{*+}}$	$.0151 \pm .0012(stat)$	$.0054 \pm .0007(stat)$	$.0086 \pm .0019(stat)$
$\sigma_{D^{*+}}$, pb	$457 \pm 64(stat) \pm 38(MC)$	$440 \pm 98(stat) \pm 55(MC)$	$464 \pm 148(stat) \pm 96(MC)$
$< \sigma_{D^{*+}} >$, pb		$453 \pm 58(stat) \pm 80(syst)$	

To choose the Monte Carlo generator describes the data better we compare the p_T, W_{vis} and $x_E = E_{D^{*+}}/E_{vis}$ distributions (Fig. 5) for D^{*+} candidates with the PYTHIA and TWOGAM prediction.

The Monte Carlo distributions are normalized to the integrated luminosity. There is no significant disagreement between data and distributions for both MC generator programs. Although PYTHIA describes the data slightly better, we cannot fix the MC generator studying the kinematical distributions of D^{*+} candidates.

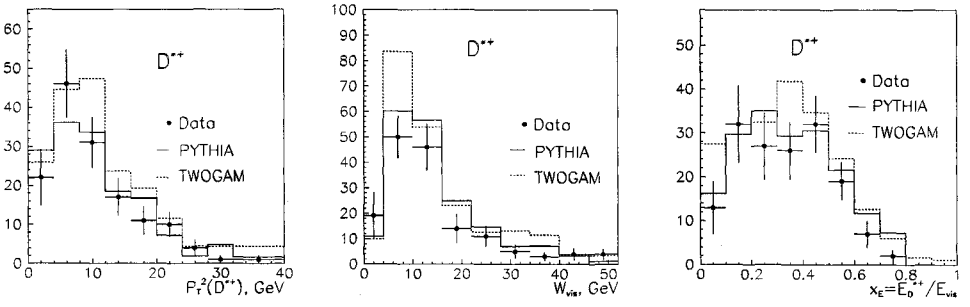

FIGURE 5. p_T momentum, W_{vis} and $x_E = E_{D^{*+}}/E_{vis}$ distributions for D^{*+} candidates are compared with the PYTHIA and TWOGAM predictions. The Monte Carlo distributions are normalized to the integrated luminosity.

The study of D^{*+} meson production in the $\gamma\gamma$ events with the requirement that at least one charged track have $p_T > 1.2$ GeV/c in the whole range of polar angle and comparison of $\sigma_{D^{*+}}$ for different cuts indicate that PYTHIA also describes better the relation of both cross sections.

D^0, D^+, AND Λ_c PRODUCTION

D^0

The D^0 were detected by their decay into $K^-\pi^+$. The large combinatorial background prohibits observation of a signal of the D^0 in the decay mode $D^0 \to K^-\pi^+\pi^-\pi^+$. For the D^0 candidates, all combinations of pairs of oppositely charged kaon and pion were used.

All charged particles satisfing the

kaon criterion with $x_K > 0$ were taken as the kaon. All charged tracks not identified as electron, muon or kaon were assumed to be pions.

The invariant $K^-\pi^+$ mass distribution is shown in Fig. 6. A clear D^0 peak is observed.

The histogram was fitted by the sum of a Gaussian function and a polynomial background. The observed number of events in the signal (N_{obs}), reconstruction efficiency (ε_{sel}) and calculated cross section (σ_{D^0}) are presented in Table 3.

The systematic uncertainties (Table 3) include the contributions from the reconstruction efficiency and branching fractions added in quadrature.

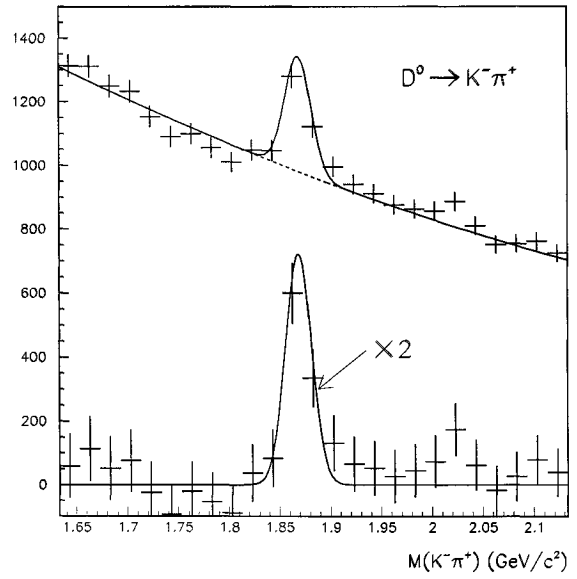

FIGURE 6. The invariant $K^-\pi^+$ mass distribution. The histogram is fitted by the sum of a Gaussian function and a polynomial background. The mass distribution scaled by a factor of 2 after background subtraction is also shown.

D^+

The D^+ were detected by their decay into $K^-\pi^+\pi^+$. All combinations of a charged kaon and two pions with charges opposite to the kaon charge were considered.

The kaon candidates were required to satisfy the "tight" kaon selection $x_K > 0.75$.

The invariant $K^-\pi^+\pi^+$ mass distribution is shown in Fig. 7. A clear D^+ peak is seen.

The histogram was fitted by the sum of a Gaussian function and a polynomial background. The observed number of events in the signal, the reconstruction efficiency and calculated cross section of the inclusive D^+ production are presented in Table 3.

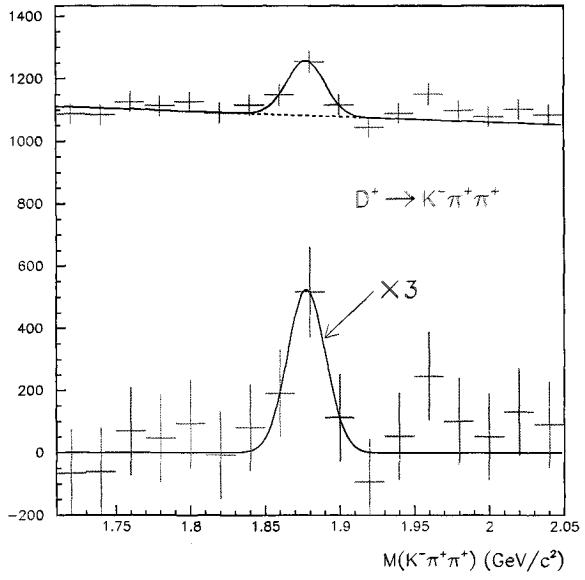

FIGURE 7. The invariant $K^-\pi^+\pi^+$ mass distribution. The histogram is fitted by the sum of a Gaussian function and a polynomial background. The mass distribution scaled by a factor of 3 after background subtraction is also shown.

Λ_c

The Λ_c is detected in the decay channels $pK^-\pi^+$, $\Lambda\pi^+\pi^-\pi^+$, pK^0_s, $pK^0_s\pi^+\pi^-$, $pK^-\pi^+\pi^0$ and $\Lambda\pi^+\pi^0$.

For proton identification the "proton net" from the MACRIB package was used. As proton candidates, the charged particles satisfing the "tight" proton criterion

$x_p > 0.75$ were used. For charged kaons one also required $x_K > 0.75$. The K_s^0 and Λ were reconstructed with the standard fitting procedure of the the secondary vertex [21]. For the proton from the Λ decay the "loose" proton criterion $x_p > -0.5$ was required. Two photons were considered as the π^0, if

- both photons were converted before TPC with an invariant mass of

$$0.115 \text{ GeV/c}^2 < M_{\gamma\gamma} < 0.155 \text{ GeV/c}^2;$$

- one or both photons were measured in the HPC with the invariant mass of

$$0.100 \text{ GeV/c}^2 < M_{\gamma\gamma} < 0.170 \text{ GeV/c}^2.$$

The Λ_c invariant mass distribution for the sum of all considered decay channels was shown in Fig. 8. The Λ_c signal is clearly observed.

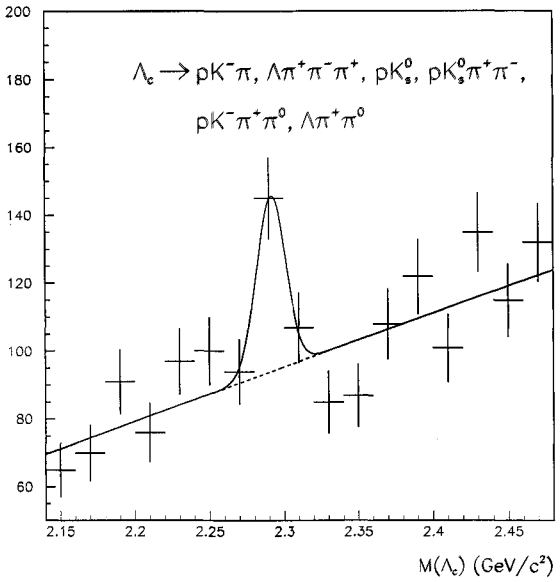

FIGURE 8. The sum of the invariant mass distributions of the $pK^-\pi^+$, $\Lambda\pi^+\pi^-\pi^+$, pK_s^0, $pK_s^0\pi^+\pi^-$, $pK^-\pi^+\pi^0$ and $\Lambda\pi^+\pi^0$ systems. The histogram was fitted by the sum of a Gaussian function and a polynomial background.

The histogram was fitted by the sum of a Gaussian function and a polynomial background. The observed number of events in signal, reconstruction efficiency and cross section of the inclusive Λ_c production are presented in Table 3.

TABLE 3. Calculation of the cross sections of the processes $e^+e^- \to e^+e^- D^0(D^+, \Lambda_c)X$.

	D^0	D^+	Λ_c
N_{obs}	498 ± 74	277 ± 66	62 ± 26
ε_{sel}	$.0325 \pm .0022(stat)$	$.0196 \pm .0024(stat)$	$.012 \pm .003(stat)$
$\sigma_{D,(\Lambda_c)}$ (pb)	$918 \pm 136(stat) \pm 62(MC)$ $\pm 157(syst)$	$362 \pm 86(stat) \pm 45(MC)$ $\pm 62(syst)$	$85 \pm 42(stat)$ $\pm 14(syst)$

To compare the production of different charm mesons we estimated the inclusive cross sections of D^0 and D^+ direct production. The inclusive cross section of D^0 production can be written as

$$\sigma_{D^0} = \sigma_{D^0}^{direct} + \sigma_{D^{*0}} + Br(D^{*+} \to D^0 + X) \cdot \sigma_{D^{*+}},$$

where $\sigma_{D^0}^{direct}$ is the inclusive cross section of the direct D^0 production, $\sigma_{D^{*0(+)}}$ is the inclusive cross section of the $D^{*0(+)}$ production, $Br(D^{*+} \to D^0+X)$ is the branching fraction of the decay $D^{*+} \to D^0 + X$. With $Br(D^{*+} \to D^0 + X) = .683$ [27] and under the assumption that $\sigma_{D^{*0}} \simeq \sigma_{D^{*+}}$ we have the following estimation: $\sigma_{D^0}^{direct} = 156 \pm 178$ pb. We took into account only statistical errors since we expect that systematic effects shift all the charm state cross sections in the same way and that for the cross section ratios it can be neglected.

For D^+ meson production we have the following relation:

$$\sigma_{D^+} = \sigma_{D^+}^{direct} + Br(D^{*+} \to D^+ + X) \cdot \sigma_{D^{*+}},$$

where $Br(D^{*+} \to D^+ + X) = .317$ [27]. The value $\sigma_{D^+}^{direct} = 218 \pm 99$ pb was obtained from the previous relation. The value of the $\sigma_{D^+}^{direct}$ and $\sigma_{D^0}^{direct}$ error is overestimated here because the correlation of $\sigma_{D^{+(0)}}$ and $\sigma_{D^{*+}}$ values is not taken into account. Within the errors $\sigma_{D^0}^{direct} \simeq \sigma_{D^+}^{direct}$.

For the D^{*+} and D^+ mesons production we have the ratio $\sigma_{D^{*+}}/\sigma_{D^+}^{direct} = 2.1^{+2.4}_{-0.9}$.

The calculated values of cross sections of the inclusive D mesons production are consistent within errors with the (2J+1)-relation $\sigma_{D^{*+}} = 3 \cdot \sigma_{D^0} = 3 \cdot \sigma_{D^+}$.

$C\bar{C}$ PRODUCTION CROSS SECTION

In calculating the cross section, $\sigma(\gamma\gamma \to c\bar{c})$, of charm pair production in two photon collisions we used

$$\sigma(\gamma\gamma \to D^{*+}X) = 2 \times \sigma(\gamma\gamma \to c\bar{c}) \times P_{c \to D^{*+}}.$$

Here $P_{c \to D^{*+}} = (0.255 \pm 0.017)$ is the probability of a charm quark fragmentation into D^{*+} measured by DELPHI [28] in Z^0 decays into $c\bar{c}$. Because we have no experimental measurements of the $P_{c \to D^{0(+)}(\Lambda_c)}$ and because the statistical errors of the inclusive cross sections of Λ_c and direct D^0, D^+ production are rather large, we use only D^{*+} data for the $\sigma(\gamma\gamma \to c\bar{c})$ calculation.

The measured cross section of charm quark production in two photon collisions

$$\sigma(\gamma\gamma \to c\bar{c}) = 889 \pm 128(stat) \pm 157(syst) \text{ pb}$$

agrees with theoretical predictions [8] and the OPAL [19] result and is lower than the L3 [18] value.

CONCLUSIONS

A measurement of the cross section for D^{*+}, D^0, D^+ and Λ_c inclusive production in $\gamma\gamma$ collisions at LEP-II energies has been performed.

The measured cross section values and event distributions are compatible with the QCD calculations with contributions from the resolved processes, which are sensitive to the gluon density in the photon. The measured values for the inclusive cross sections are

$$\sigma(e^+e^- \to e^+e^-D^{*+}X) = 453 \pm 58(stat) \pm 80(syst) \text{ pb},$$

$$\sigma(e^+e^- \to e^+e^-D^0X) = 918 \pm 149(stat) \pm 157(syst) \text{ pb},$$

$$\sigma(e^+e^- \to e^+e^-D^+X) = 362 \pm 97(stat) \pm 62(syst) \text{ pb},$$

$$\sigma(e^+e^- \to e^+e^-\Lambda_cX) = 85 \pm 42(stat) \pm 14(syst) \text{ pb}.$$

The estimated total cross section of the charm quark production in two-photon collisions at LEP-II energies is

$$\sigma(e^+e^- \to e^+e^-c\bar{c}) = 889 \pm 128(stat) \pm 157(syst) \text{ pb}.$$

The last result agrees with theoretical predictions.

ACKNOWLEDGEMENTS

We would like to thank V.B. Anykeyev, S. Todorova-Nova, I.A. Tyapkin for fruitful discussions on this work.

REFERENCES

1. J.J. Sakurai and D. Schildknecht, Phys. Lett. **B40** (1979) 121;
   I.F. Ginzburg and V.G. Serbo, Phys. Lett. **B109** (1982) 231.
2. S.J. Brodsky, T. Kinoshita and H. Terazawa, Phys. Rev. **D4** (1971) 1532.
3. S.J. Brodsky, T.A. DeGrand, J.F. Gunion and J.H.Weis, Phys. Rev. Lett. **41** (1978) 672; Phys. Rev. **D19** (1979) 1418.
4. D.W. Duke and J.F. Owens, Phys. Rev. **D26** (1982) 1600.
5. M. Drees and K. Grassie, Z. Phys. **C28** (1985) 451.

6. H. Abramovicz, K. Charchula and A. Levy, Phys. Lett. **B269** (1991) 458.
7. M. Glück, E.Reya and A. Vogt, Phys. Rev. **D46** (1992) 1973.
8. M. Drees, M. Krämer, J. Zunft and P.M. Zerwas, Phys. Lett. **B306** (1993) 371.
9. M. Drees and R. Godbole, Nucl. Phys. **B339** (1990) 355.
10. W. Bartel *et al.*, JADE Collab., Phys. Lett. **B184** (1987) 288.
11. M. Alston-Garnjost *et al.*, TPC/2γ Collab., Phys. Lett. **B252** (1990) 499.
12. W. Braunschweig *et al.*, TASSO Collab., Z. Phys. **C47** (1990) 499.
13. R. Enomoto *et al.*, TOPAZ Collab., Phys. Rev. **D50** (1994) 1879.
14. R. Enomoto *et al.*, TOPAZ Collab., Phys. Lett. **B328** (1994) 535.
15. S. Uehara *et al.*, VENUS Collab., Z. Phys. **C63** (1994) 213.
16. T. Aso *et al.*, AMY Collab., Phys. Lett. **B363** (1995) 249;
    Phys. Lett. **B381** (1996) 372.
17. D. Buskulic *et al.*, ALEPH Collab., Phys. Lett. **B355** (1995) 595.
18. M. Acciarri *et al.*, L3 Collab., Phys. Lett. **B453** (1999) 83;
    L3 Collab., "Measurement of Charm and Beauty Production in $\gamma\gamma$ Collisions at LEP", submitted to the Intern. Europhys. Conference HEP 99, Tampere, Finland, 15-21 July 1999.
19. G. Abbiendi *et al.*, OPAL Collab., "Inclusive Production of $D^{*\pm}$ Mesons in Photon-Photon Collisions at $\sqrt{s_{ee}}$=183 and 189 GeV and First Measurement of $F_{2,c}^{\gamma}$", preprint CERN-EP/99-157 (November 1999), submitted to Eur. Phys. J. C.
20. P. Aarnio *et al.*, DELPHI Collab., Nucl. Inst. Meth. **A303** (1991) 233.
21. P. Abreu *et al.*, DELPHI Collab., Nucl. Inst. Meth. **A378** (1996) 57.
22. V. Canale *et al.*, "The DELPHI Trigger System at LEP200", DELPHI/99-7 DAS 188 (22 February 1999).
23. S. Nova, A. Olshevski and T. Todorov, "MONTE CARLO Event Generator for Two Photon Physics", DELPHI/90-35 (November 1990).
24. T. Sjöstrand, Comput. Phys. Comm. **82** (1994) 74.
25. M. Battaglia, P.M. Kluit, "Particle identification using the RICH detectors based on the RIBMEAN package", DELPHI/96-133 (September 1996);
    W. Adam *et al.*, " Analysis techniques for the DELPHI ring imaging Cherenkov detector", DELPHI/94-112 (June 1994).
26. Z. Albrecht, M. Feindt and M. Moch, "MACRIB. High efficiency - high purity hadron identification for DELPHI", DELPHI/99-150 (October 1999).
27. Review of Particle Physics, Eur. Phys. J. **C15** (2000) 1.
28. P. Abreau *et al.*, DELPHI Collab., Eur. Phys. J. **C12** (2000) 209.